

# Synthesis of tri-block copolymers through reverse atom transfer radical polymerization of methyl methacrylate using polyurethane macroiniferter

H. Verma, T. Kannan\*

Department of Chemistry, University of Delhi, North Campus, Delhi – 110 007, India

Received 28 May 2008; accepted in revised form 9 July 2008

**Abstract.** Reverse atom transfer radical polymerization was successfully used for the first time to synthesis tri-block copolymers. Poly (methyl methacrylate)-*block*-polyurethane-*block*-poly (methyl methacrylate) tri-block copolymers were synthesized using tetraphenylethane-based polyurethane as a macroiniferter, copper(II) halide as a catalyst and *N, N, N', N'', N''*-pentamethyldiethylenetriamine as a ligand. Controlled nature of the polymerization was confirmed by the linear increase of number average molecular weight with increasing conversion. Mole contents of poly (methyl methacrylate) present in the tri-block copolymers were calculated using proton nuclear magnetic resonance spectroscopy and the results were comparable with the gel permeation chromatography results. Differential scanning calorimetric results confirmed the presence of two different types of blocks in the tri-block copolymers.

**Keywords:** polymer synthesis, molecular engineering, atom transfer radical polymerization, tri-block copolymers, polyurethane, poly(methyl methacrylate)

## 1. Introduction

Living polymerization remains the main tool to synthesize diverse homopolymers and block copolymers of predetermined molecular weight and composition [1–3]. Controlled radical polymerization (CRP) [4–11] is another tool to improve chemoselectivity of radical polymerization. Atom transfer radical polymerization (ATRP) is the most robust CRP method to synthesize different types of polymers because of its simple polymerization conditions [12, 13]. In ATRP, simple and easily available chemicals such as organic halides and transition metal halides in their lower oxidation state are used as initiators and catalysts respectively [14, 15]. Besides their innumerable advantages, the major disadvantage of this normal ATRP is toxicity of the initiator and easy oxidation of the catalyst [16]. To overcome these difficulties Wang and

Matyjaszewski proposed reverse ATRP as an alternative to normal ATRP [17]. Reverse ATRP differs from normal ATRP in its initiation process. In the case of initiators, organic halides are used in normal ATRP whereas conventional radical initiators such as peroxide or azo compounds are used in reverse ATRP. Similarly, in the case of catalysts, more stable transition metal halides in their higher oxidation state are used in reverse ATRP whereas less stable transition metal halides in their lower oxidation state are used in normal ATRP [17]. Monomers such as styrene [17], methyl methacrylate [18, 19] and methyl acrylate [17, 20] were successfully polymerized through reverse ATRP using conventional initiators such as benzoyl peroxide and 2,2'-azobis(isobutyronitrile). But these initiators cannot undergo reversible deactivation and due to this, the concentration of the primary radicals is

\*Corresponding author, e-mail: [tharani@chemistry.du.ac.in](mailto:tharani@chemistry.du.ac.in)  
© BME-PT and GTE

very high even in the presence of strong deactivators such as  $\text{CuCl}_2$  especially at the early stage polymerization [17]. To overcome this, recently iniferters (*initiator-transfer agent-terminator*) were used instead of conventional initiators.

1,1,2,2-Tetraphenylethane-1,2-diol (TPED) is a well known radical initiator for the polymerization of vinyl monomers [21]. Though it contains a well known tetraphenylethane iniferter group in its structure, it doesn't act as an iniferter in controlled radical polymerization. This is due to the formation of benzophenone and monomer free radical in the initiation step. Due to this reason, the initiation mechanism of TPED is different from other tetraphenylethane derivatives [22]. 1,1,2,2-Tetraphenyl-1,2-dicyanoethane (TPDE) polymerizes vinyl monomer through controlled radical polymerization. As a result, TPDE acts as an iniferter whereas TPED neither acts as an iniferter nor follows controlled radical polymerization [22]. If the  $-\text{OH}$  groups of TPED are modified it can also act as an iniferter. Hence in the present investigation the hydroxyl groups of TPED have been modified by reacting it with NCO terminated polyurethane and the resulting polyurethane-based macroiniferter (PU-TPE) is used in reverse ATRP. Iniferter-based reverse ATRP initiating systems such as diethyl-2,3-dicyano-2,3-diphenylsuccinate/ $\text{FeCl}_3$ /triphenylphosphine ( $\text{PPh}_3$ ) [23], 2,3-dicyano-2,3-di(*p*-tolyl)succinate/ $\text{CuCl}_2$ /bpy [24], 1,1,2,2-tetraphenyl-1,2-ethanediol (TPED)/ $\text{FeCl}_3$ / $\text{PPh}_3$  [16, 25], tetraethylthiuram disulphide/ $\text{CuBr}$ /bpy [26] were successfully used to polymerize vinyl and acrylate monomers. These initiating systems lower the concentration of primary radicals in the initiating step as in the case of normal ATRP. Unlike organic iniferters, macroiniferters were not used in reverse ATRP so far by any research group. Though multi-block copolymers were synthesized through macroiniferters [27–29], there was no report on the synthesis of tri-block copolymers through reverse ATRP. In fact, Matyjaszewski reported in his review that tri-block copolymers cannot be synthesized through reverse ATRP [30]. Hence in the present investigation, for the first time, synthesis of poly(methyl methacrylate)-*block*-polyurethane-*block*-poly(methyl methacrylate) (PMMA-*b*-PU-*b*-PMMA) tri-block copolymers through reverse ATRP is reported. During this study, tetraphenylethane containing polyurethane was used as a

macroiniferter, cupric halide ( $\text{CuBr}_2$  or  $\text{CuCl}_2$ ) was used as a catalyst and *N, N, N', N'', N'''*-pentamethyldiethylenetriamine (PMDETA) was used as a ligand to polymerize methyl methacrylate.

## 2. Experimental section

### 2.1. Materials

Toluene diisocyanate (TDI; mixture of 80% 2,4 and 20% 2,6-TDI isomers), dibutyltin dilaurate (DBTDL), calcium hydride, and PMDETA were used as received from Aldrich, U.S.A. Acetonitrile, benzophenone,  $\text{CuBr}_2$  and  $\text{CuCl}_2$  were used as received from CDH, India. Analytical grade *N, N*-dimethylformamide (DMF; CDH, India) was distilled under reduced pressure and the middle portions were used after storing over type 4 Å molecular sieves. The inhibitor present in methyl methacrylate (MMA; CDH, India) was removed using a conventional method. It was then distilled under reduced pressure and the middle portion was stored at  $0-4^\circ\text{C}$  until use. Poly(tetramethyleneoxide) glycol of molecular weight 1000 (PTMG; Aldrich, USA) was purified by heating at  $105^\circ\text{C}$  under reduced pressure for 3 h just before use. All other chemicals were of analytical grades and were used as received.

### 2.2. Synthesis of TPED and tetraphenylethane-based polyurethane macroiniferter (PU-TPE)

TPED was prepared from benzophenone and 2-propanol as reported in the literature [22]. PU-TPE was synthesized based on the reported method using one mole of PTMG, two moles of TDI and one mole of TPED [27–29]. Here the completion of the reaction between NCO and OH was monitored and confirmed using Fourier-transform infrared (FT-IR) spectroscopy. The peak corresponds to NCO group was observed at  $2264\text{ cm}^{-1}$ . This peak was gradually reduced and at the end of the reaction this peak was completely disappeared.

### 2.3. Reverse ATRP of MMA using PU-TPE/ $\text{CuX}_2$ /PMDETA initiating system

For the polymerization of MMA, first PU-TPE was dissolved in DMF and known quantity of

PMDETA,  $\text{CuX}_2$  ( $\text{X} = \text{Br}$  or  $\text{Cl}$ ) and MMA were added successively. The homogeneous reaction mixture was degassed by three alternate freeze-pump-thaw cycles, sealed under vacuum and placed in a thermo-stated oil bath controlled to  $\pm 0.01^\circ\text{C}$  for selected time. At the end of the stipulated period of time, the reaction mixture was removed from the oil bath and the reaction was arrested by dipping in an ice-salt mixture. The resulting solution was poured into a 10-fold excess of methanol and the precipitate was filtered using sintered-glass crucible, washed with methanol and dried in vacuum. The dried samples were washed thoroughly with acetone and acetonitrile to remove traces of homo PU and homo PMMA respectively. The resulting pure block copolymers were dried in vacuum and weighed.

## 2.4. Characterization

Number-average ( $\bar{M}_n$ ) and weight-average ( $\bar{M}_w$ ) molecular weights and molecular weight distribution (MWD) were determined by gel permeation chromatography (GPC) using polymer laboratories GPC 50 integrated system equipped with differential refractometer (RI Detector) and PLgel 5  $\mu\text{m}$  MIXED-C column. Tetrahydrofuran was used as an eluent at a flow rate of 1.0 ml/min and the molecular weight calibrations were done using polystyrene standards. Differential scanning calorimetry (DSC) was carried out using DSC Q200 instrument (TA instruments, USA) at a heating rate of  $10^\circ\text{C}/\text{min}$  under  $\text{N}_2$  atmosphere and thermo gravimetric analysis (TGA) was carried out using DTG-60 instrument (Shimadzu, Japan) at a heating rate of  $10^\circ\text{C}/\text{min}$  under  $\text{N}_2$  atmosphere. Fourier-transform nuclear magnetic resonance (FT-NMR) spectra were recorded on a Bruker DPX-300 NMR instru-

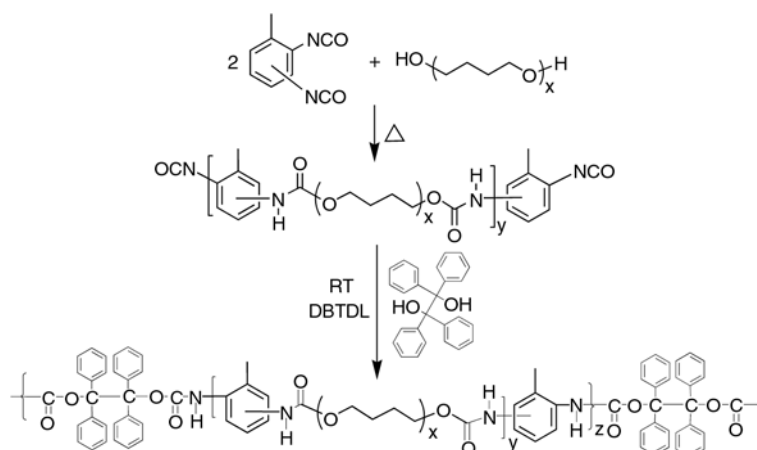


**Figure 1.** Synthesis of PU-TPE

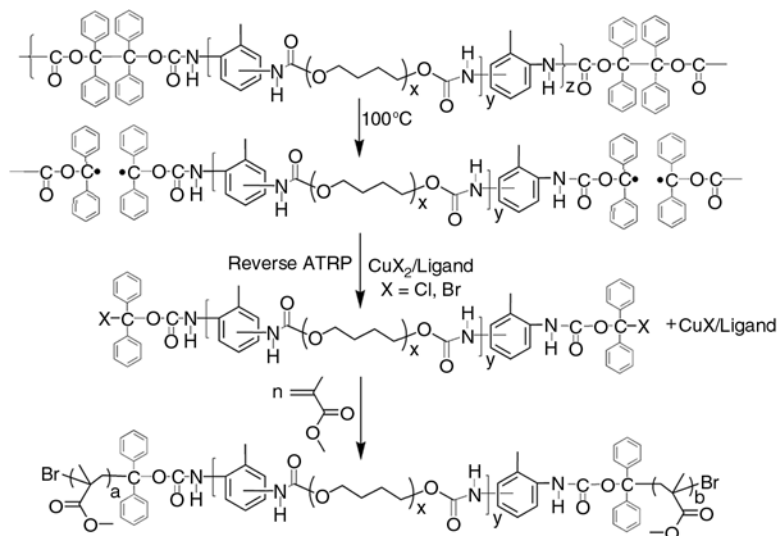


**Figure 2.** Synthesis of PMMA-*b*-PU-*b*-PMMA tri-block copolymers through reverse ATRP

ment using deuterated dimethyl sulfoxide as the solvent and tetramethylsilane as the internal standard. FT-IR spectra were recorded as KBr pellets on a Nicolet Impact 400 FT-IR spectrophotometer.

### 3. Results and discussion

Figure 1 and Figure 2 show the synthetic route for the preparation of PU-TPE macroiniferter and PMMA-*b*-PU-*b*-PMMA tri-block copolymers respectively. Here the concentration of PU-TPE was calculated using number of TPE groups present in PU-TPE using  $\overline{M}_n$  obtained from GPC (cf. Tables 1 and 2). Since PU-TPE formed two radicals in the initiation step, the ratio of PU-TPE, CuX<sub>2</sub> (X = Br or Cl) and PMDETA was maintained at 1:2:2 respectively. To select the polymerization

temperature, initially the polymerization was carried out at 80°C, but there was no polymerization and the polymerization was sluggish at 90°C. However, in the case of the polymerization at 100°C, the reaction was not sluggish and hence 100°C was chosen as a polymerization temperature for the present investigation. DMF was chosen as a solvent as it was good solvent for PU-TPE macroiniferter.

#### 3.1. Mechanism of polymerization

To understand the mechanism of polymerization, effect of changing time on the polymerization of MMA was carried out and the results are presented in Tables 1 and 2. Here, for the calculation of conversion, weight of [MMA]<sub>0</sub> was considered and weight of [PU-TPE]<sub>0</sub> was not considered as there

**Table 1.** Effect of time on reverse ATRP of MMA using CuCl<sub>2</sub> at 100°C

Code No.	Time [h]	Conversion <sup>a</sup> [%]	Molar content of PMMA <sup>b</sup> [%]	$\overline{M}_n \cdot 10^{-3}$ [th] <sup>c</sup>	GPC results			f <sup>d</sup>
					$\overline{M}_n \cdot 10^{-3}$	$\overline{M}_w \cdot 10^{-3}$	$\overline{M}_w/\overline{M}_n$	
PU-TPE	0	0	0	–	20.0	29.8	1.49	–
TBCP 1	1	3.5	21.2	21.4	23.5	44.8	1.91	0.90
TBCP 2	3	8.7	50.1	23.5	28.7	53.0	1.85	0.81
TBCP 3	6	15.7	62.3	26.3	31.0	55.1	1.78	0.84
TBCP 4	9	21.0	76.2	28.4	34.2	58.4	1.71	0.83
TBCP 5	12	26.3	92.1	30.5	37.4	61.7	1.65	0.81
TBCP 6	18	33.3	106.7	33.3	40.0	63.2	1.58	0.83

<sup>a</sup>conversion determined gravimetrically

<sup>b</sup>molar content of PMMA was calculated by comparing integration values of the peaks derived from PTMO and –CH<sub>3</sub> protons of PMMA blocks on <sup>1</sup>H NMR spectra [33]

<sup>c</sup> $\overline{M}_{n,th} = \{([MMA]_0/2[PU-TPE]) \times \text{monomer conversion}\} + \text{molecular weight of PU-TPE}$

<sup>d</sup> $f = \overline{M}_{n,th} / \overline{M}_{n,GPC}$

Polymerization conditions: [PU-TPE]<sub>0</sub> = 0.288 mmol; [PMDETA]<sub>0</sub> = [CuCl<sub>2</sub>]<sub>0</sub> = 0.576 mmol; [MMA]<sub>0</sub> = 57.6 mmol; 5.94 ml of DMF solution.

**Table 2.** Effect of time on reverse ATRP of MMA using CuBr<sub>2</sub> at 100°C

Code No.	Time [h]	Conversion <sup>a</sup> [%]	Molar content of PMMA <sup>b</sup> [%]	$\overline{M}_n \cdot 10^{-3}$ [th] <sup>c</sup>	GPC results			f <sup>d</sup>
					$\overline{M}_n \cdot 10^{-3}$	$\overline{M}_w \cdot 10^{-3}$	$\overline{M}_w/\overline{M}_n$	
PU-TPE	0	0	0	–	20.0	29.8	1.49	–
POLY 1	1	6.0	28.9	22.4	24.6	54.1	2.20	0.91
POLY 2	3	13.8	56.2	25.5	29.8	60.8	2.04	0.85
POLY 3	6	22.5	72.1	29.0	33.2	64.7	1.95	0.87
POLY 4	9	31.2	96.2	32.5	37.9	70.5	1.86	0.85
POLY 5	12	39.9	114.1	35.9	41.0	73.3	1.79	0.87
POLY 6	18	52.9	154.7	41.1	49.0	83.8	1.71	0.84

<sup>a</sup>conversion determined gravimetrically

<sup>b</sup>molar content of PMMA was calculated by comparing integration values of the peaks derived from PTMO and –CH<sub>3</sub> protons of PMMA blocks on <sup>1</sup>H NMR spectra [33]

<sup>c</sup> $\overline{M}_{n,th} = \{([MMA]_0/2[PU-TPE]) \times \text{monomer conversion}\} + \text{molecular weight of PU-TPE}$

<sup>d</sup> $f = \overline{M}_{n,th} / \overline{M}_{n,GPC}$

Polymerization conditions: [PU-TPE]<sub>0</sub> = 0.288 mmol; [PMDETA]<sub>0</sub> = [CuBr<sub>2</sub>]<sub>0</sub> = 0.576 mmol; [MMA]<sub>0</sub> = 57.6 mmol; 5.94 ml of DMF solution.

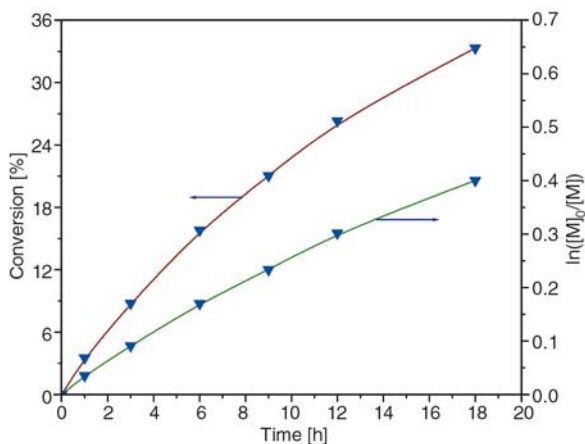


**Figure 3.** Time-conversion and time- $\ln([M]_0/[M])$  plots for the polymerization of MMA at 100°C using PU-TPE/PMDETA/CuCl<sub>2</sub> initiating system. [PU-TPE]<sub>0</sub> = 0.288 mmol; [PMDETA]<sub>0</sub> = [CuCl<sub>2</sub>]<sub>0</sub> = 0.576 mmol; [MMA]<sub>0</sub> = 57.6 mmol; 5.94 ml of DMF solution.

was no change of weight of PU-TPE during the change of polymerization time. Figure 3 presents the kinetics of the polymerization of MMA at 100°C initiated by PU-TPE/CuCl<sub>2</sub>/PMDETA initiating system. The straight line obtained in time- $\ln([M]_0/[M])$  plot indicates that the concentration of growing radicals was steady throughout the polymerization. Moreover, as shown in Figure 4,  $\bar{M}_{n,GPC}$ , number average molecular weight from GPC, increases with increasing monomer conversion which is a clear evidence for the ‘living’ nature of the PU-TPE/CuCl<sub>2</sub>/PMDETA initiating system. Maximum conversion obtained for the PU-TPE/

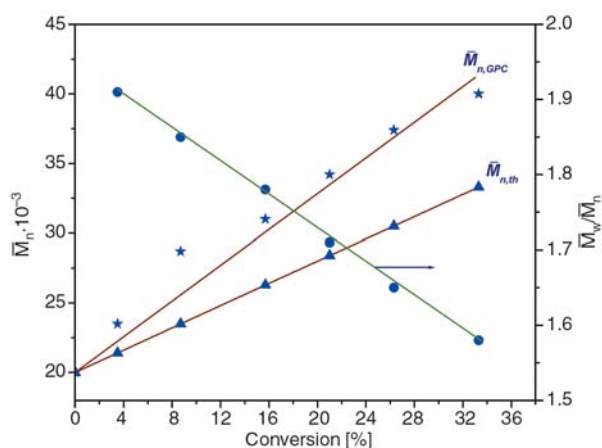


**Figure 4.** Conversion- $\bar{M}_n$  and conversion- $\bar{M}_w/\bar{M}_n$  plots for the polymerization of MMA at 100°C using PU-TPE/PMDETA/CuCl<sub>2</sub> initiating system. [PU-TPE]<sub>0</sub> = 0.288 mmol; [PMDETA]<sub>0</sub> = [CuCl<sub>2</sub>]<sub>0</sub> = 0.576 mmol; [MMA]<sub>0</sub> = 57.6 mmol; 5.94 ml of DMF solution.

CuCl<sub>2</sub>/PMDETA initiating system was 33.3% and  $\bar{M}_n$  of the tri-block copolymers reached upto 40 000 at 18 h (Table 1, TBCP 6). MWD of the tri-block copolymers was fairly narrow (Table 1, 1.91–1.58) and became narrower as conversion increases. Apparent initiator efficiency ( $f = \bar{M}_{n,th} / \bar{M}_{n,GPC}$ , where  $\bar{M}_{n,th}$  denotes theoretical number average molecular weight) of PU-TPE/CuCl<sub>2</sub>/PMDETA initiating system was also calculated and it was found to be high for TBCP 1 (Table 1, 0.90) and low for TBCP 2 and TBCP 5 (Table 1, 0.81). Apparent initiator efficiency,  $f$ , describes the intrinsic efficiency of the initiator and its value gives us an idea about the extent of unavoidable radical-radical irreversible termination reactions are taking place in a particular polymerization reaction. The low  $f$  value shows the presence of more irreversible termination reactions [31].

To study the effect of nature of the catalyst, CuBr<sub>2</sub> was used instead of CuCl<sub>2</sub> for the polymerization of MMA and the results are presented in Table 2. Similar to the previous system, PU-TPE/CuBr<sub>2</sub>/PMDETA initiating system also shows ‘livingness’ during the formation of the tri-block copolymers. Figures 5 and 6 present time-vs-conversion-vs- $\ln([M]_0/[M])$  and conversion-vs- $\bar{M}_n$ -vs-MWD plots for TPE-PU/CuBr<sub>2</sub>/PMDETA initiating system respectively. Maximum conversion obtained in this case was 52.9% and  $\bar{M}_n$  was 49 000 at 18 h (Table 2, POLY 6). Initiator efficiency was also

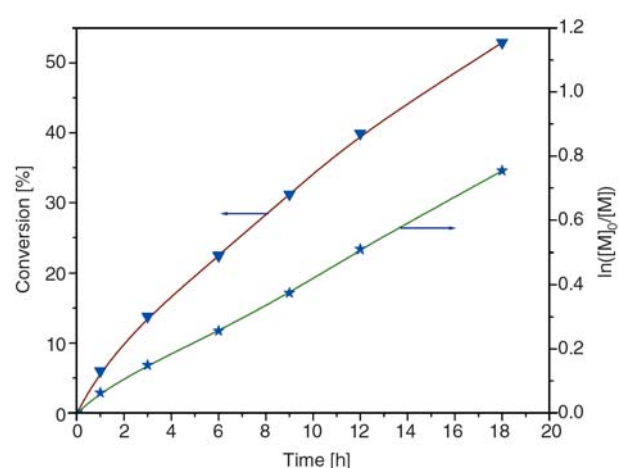


**Figure 5.** Time-conversion and time- $\ln([M]_0/[M])$  plots for the polymerization of MMA at 100°C using PU-TPE/PMDETA/CuBr<sub>2</sub> initiating system. [PU-TPE]<sub>0</sub> = 0.288 mmol; [PMDETA]<sub>0</sub> = [CuBr<sub>2</sub>]<sub>0</sub> = 0.576 mmol; [MMA]<sub>0</sub> = 57.6 mmol; 5.94 ml of DMF solution.

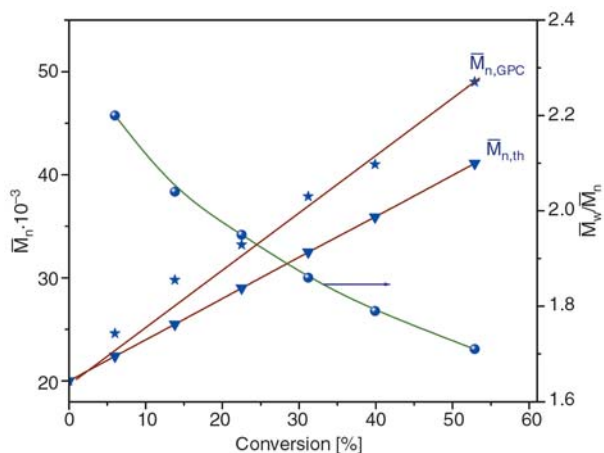


**Figure 6.** Conversion- $\bar{M}_n$  and conversion- $\bar{M}_w/\bar{M}_n$  plots for the polymerization of MMA at 100°C using PU-TPE/PMDETA/CuBr<sub>2</sub> initiating system. [PU-TPE]<sub>0</sub> = 0.288 mmol; [PMDETA]<sub>0</sub> = [CuBr<sub>2</sub>]<sub>0</sub> = 0.576 mmol; [MMA]<sub>0</sub> = 57.6 mmol; 5.94 ml of DMF solution.

calculated for this system and it was found to be high for POLY 1 (Table 2, 0.91) and low for POLY 6 (Table 2, 0.84). The conversion in CuCl<sub>2</sub> system is lower than the CuBr<sub>2</sub> system but based on the MWD values former system is more controlled than the latter system. As R–Cl bond is more

stronger than R–Br bond, CuCl<sub>2</sub> acts as a good deactivator of the radical generated from PU-TPE than CuBr<sub>2</sub> and as a result conversion in CuCl<sub>2</sub> system was lower than the CuBr<sub>2</sub> system. There is a little lack of linearity especially in the time-vs-conversion-vs- $\ln([M]_0/[M])$  plots (Figure 3 and Figure 5) and this might be due to the lack of inefficient deactivation by CuX<sub>2</sub> (X = Cl, Br)/PMDETA complex, which lead to the irreversible radical-radical termination. However ‘living’ nature of both the initiating systems was confirmed by linear increase of  $\bar{M}_n$  with conversion plots. Moreover ‘living’ nature was further supported by the good agreement between  $\bar{M}_{n,th}$  and  $\bar{M}_{n,GPC}$  values and MWD became narrower as the conversion increases.

### 3.2. Spectral studies

The formation of PU-TPE and PMMA-*b*-PU-*b*-PMMA was confirmed by <sup>1</sup>H NMR spectroscopy. Figure 7 shows <sup>1</sup>H NMR spectra of PU-TPE and PMMA-*b*-PU-*b*-PMMA tri-block copolymer obtained at 6 h (Table 2, POLY 3). The spectral data of PU-TPE and PMMA-*b*-PU-*b*-PMMA tri-

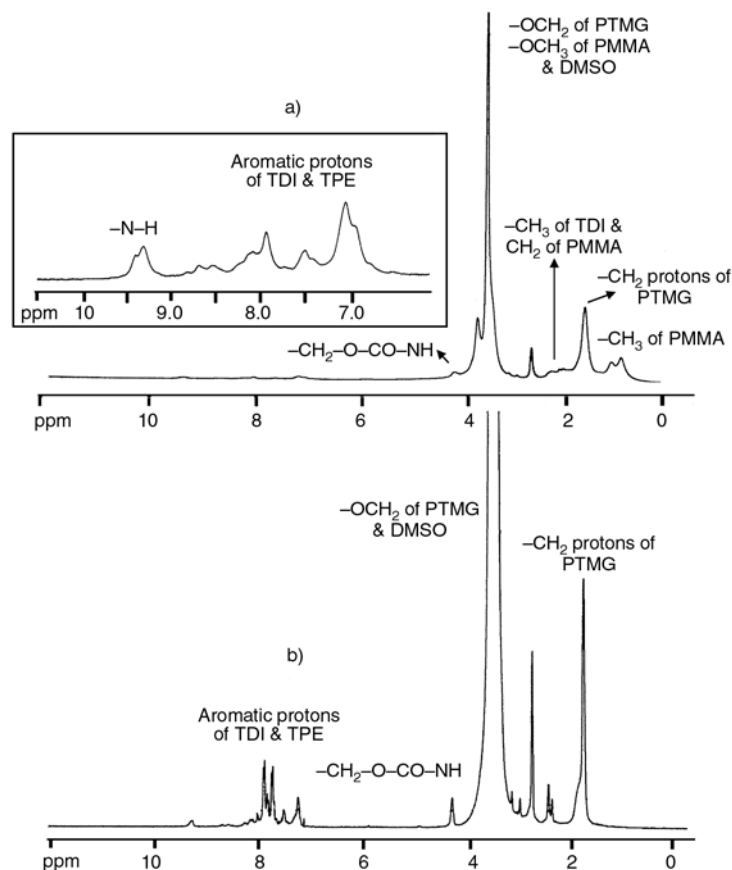


**Figure 7.** <sup>1</sup>H NMR spectra of (a) PMMA-*b*-PU-*b*-PMMA tri-block copolymer POLY 3 and (b) PU-TPE

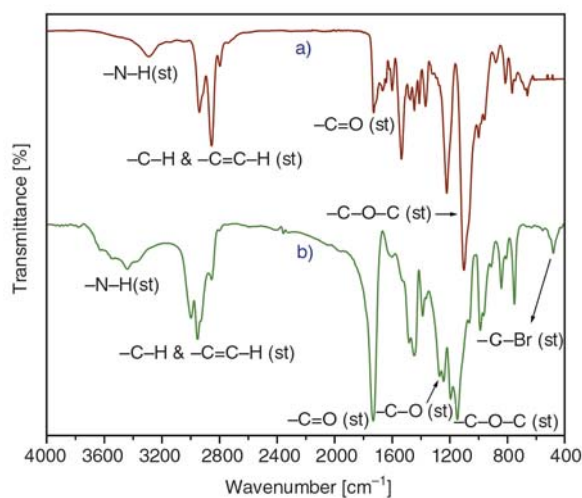
**Table 3.**  $^1\text{H}$  NMR data of PU-TPE and PMMA-*b*-PU-*b*-PMMA tri-block copolymer, POLY 3

PU-TPE		PMMA- <i>b</i> -PU- <i>b</i> -PMMA tri-block copolymer, POLY 3	
$^1\text{H}$	Chemical shift [ppm]	$^1\text{H}$	Chemical shift [ppm]
$-\text{N}-\text{H}$	8.01–9.15	$-\text{N}-\text{H}$	8.01–9.17
$\text{C}_6\text{H}_3$ of TDI, TPE	7.07–7.86	$\text{C}_6\text{H}_3$ of TDI, TPE	7.08–7.89
$\text{C}_6\text{H}_3(\text{CH}_3)\text{NH}$	2.05–2.12	$\text{C}_6\text{H}_3(\text{CH}_3)\text{NH}$ , $-\text{CH}_2$ of PMMA	1.82–2.15
$-\text{CH}_2-$ of PTMG	1.51	$-\text{CH}_2-$ of PTMG	1.53
$-\text{O}-\text{CH}_2-$ of PTMG, DMSO	3.15	$-\text{O}-\text{CH}_2-$ of PTMG, $-\text{OCH}_3$ of PMMA, DMSO	3.1–3.7
$-\text{CH}_2-\text{O}-\text{CO}-\text{NH}$	4.07	$-\text{CH}_2-\text{O}-\text{CO}-\text{NH}$	4.11
		$-\text{OCH}_3$ of PMMA	3.5
		$-\text{CH}_3$ of PMMA	0.82–1.18
		$-\text{CH}_3$ of PMMA ( <i>rr</i> )	0.82
		$-\text{CH}_3$ of PMMA ( <i>mr</i> )	1.0
		$-\text{CH}_3$ of PMMA ( <i>mm</i> )	1.18

block copolymer is given in Table 3. In the  $^1\text{H}$  NMR spectrum of PU-TPE the aromatic protons derived from TDI and TPE were merged and appeared at 7.07–7.86 ppm. The  $-\text{N}-\text{H}$  protons of urethane groups and methyl protons derived from TDI were appeared at 8.01–9.15 ppm and 2.05–2.12 ppm respectively. The peaks correspond to  $-\text{CH}_2-$  and  $-\text{OCH}_2-$  protons of PTMG resonate at 1.51 and 3.15 ppm respectively. The  $-\text{OCH}_2-$  of PTMG which is attached to urethane group appeared at 4.07 ppm. In the  $^1\text{H}$  NMR spectrum of the tri-block copolymer obtained at 6 h (Table 2, POLY 3), the  $-\text{CH}_3$  protons of PMMA resonated at 0.82, 1.00 and 1.18 ppm which correspond to syndiotactic (*rr*), atactic (*mr*) and isotactic (*mm*) PMMA respectively. The  $-\text{OCH}_3$  protons of PMMA and  $-\text{OCH}_2-$  protons of PTMG merged with DMSO and appeared between 3.1–3.7 ppm. The  $-\text{CH}_2-$  protons of PTMG present in the tri-block copolymer appeared at 1.53 ppm. The methyl protons derived from TDI and  $-\text{CH}_2-$  protons of PMMA merged and appeared at 1.82–2.15 ppm. Aromatic protons (derived from TDI and TPE groups) and  $-\text{N}-\text{H}$  protons of urethane resonated at 7.08–7.89 ppm and 8.01–9.17 ppm respectively. The  $-\text{OCH}_2-$  of PTMG present in tri-block copolymer attached to urethane group was appeared at 4.11 ppm. The tacticity ratio of PMMA in POLY 3 is *rr*:*mr*:*mm* = 54:39:7 which is more or less similar to the reported tacticity ratio of PMMA prepared by ATRP [32]. The molar content of PMMA in the tri-block copolymers can easily be found out by comparing molecular weights (obtained by GPC) of PU-TPE and tri-block copolymers which are given in Tables 1 and 2. It can also be found out by comparing peak integration ratio of  $-\text{CH}_2-\text{CH}_2-$  group

of PTMG at 1.5 ppm and methyl protons of PMMA blocks at 0.82–1.18 ppm through  $^1\text{H}$  NMR technique as described in the literature [33]. The molar content values are given in Tables 1 and 2 and these values are comparatively similar to the molar content values from GPC. Presence of peaks corresponds to PMMA blocks and PU-TPE in the  $^1\text{H}$  NMR spectrum of PMMA-*b*-PU-*b*-PMMA more likely to confirm the formation of the tri-block copolymers.

The macroiniferter and the tri-block copolymer (Table 2, POLY 3) synthesized were further characterized by FT-IR spectroscopy to confirm the structure and the spectra are shown in Figure 8. Table 4 shows the FT-IR spectral data of PU-TPE and PMMA-*b*-PU-*b*-PMMA tri-block copolymers. In the FT-IR spectrum of PU-TPE, the stretching vibrations of urethane carbonyl group is at  $1743\text{ cm}^{-1}$  and bands at  $2800\text{--}3048\text{ cm}^{-1}$  are associated with aliphatic and aromatic  $-\text{C}-\text{H}$  asymmet-

**Figure 8.** FT-IR spectra of (a) PU-TPE and (b) PMMA-*b*-PU-*b*-PMMA tri-block copolymer POLY 3

**Table 4.** FT-IR data of PU-TPE and PMMA-*b*-PU-*b*-PMMA tri-block copolymer, POLY 3

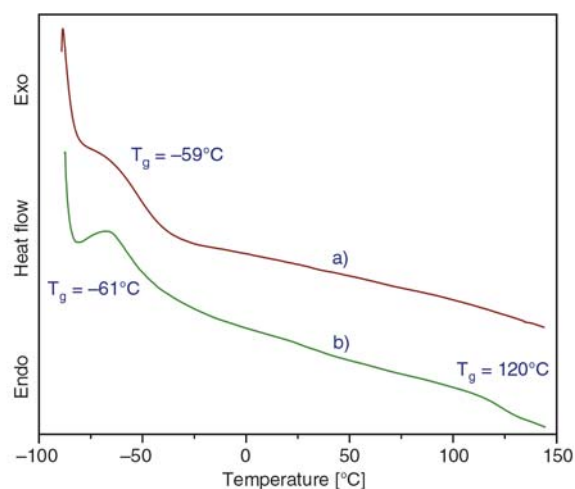
PU-TPE		PMMA- <i>b</i> -PU- <i>b</i> -PMMA tri-block copolymer, POLY 3	
Functional group	Wave number [cm <sup>-1</sup> ]	Functional group	Wave number [cm <sup>-1</sup> ]
-C=O (urethane)	1743 (st)	-C=O (NHCOO, PMMA)	1737 (st)
-C-H, -C=C-H (-CH in PU)	2800–3048 (st)	-C-H, -C=C-H (PU, PMMA)	2851–3010 (st)
-C-H (CH <sub>2</sub> in PU)	1441–1483 (bend)	-C-H (CH <sub>2</sub> in PU, PMMA)	1439–1485 (bend)
-C-H (CH <sub>3</sub> in TDI)	1371 (bend)	-C-H (CH <sub>3</sub> in TDI & PMMA)	1391 (bend)
-C-N (urethane)	1230 (st)	-C-N (urethane)	1233 (st)
-C-O-C-	1100 (st)	-C-O-C-	1136 (st)
-C=C- (TPE, TDI)	1603 (st)	-C=C- (TPE, TDI)	1660 (st)
-C=C- (TPE, TDI)	991 (bend)	-C=C- (TPE, TDI)	991 (bend)
-N-H (urethane)	3300 (st)	-N-H (urethane)	3353–3550 (st)
-N-H (urethane)	1533 (bend)	-N-H (urethane)	1528 (bend)
-C=C-H (CH in TPE, TDI)	749 (bend; out of plane)	-C=C-H (CH in TPE, TDI)	749 (bend; out of plane)
		-C-O- (ester group of PMMA)	1275 (st)
		-C-Br	490 (st)

ric and symmetric stretching vibrations present in -CH<sub>2</sub>-, -CH<sub>3</sub> groups and phenyl rings. The peak present at 1230 cm<sup>-1</sup> corresponds to -C-N- stretching vibrations present in urethane groups. The peak at 1100 cm<sup>-1</sup> is due to the stretching vibrations of ether -C-O-C- groups and stretching vibrations of -C=C- appear at 1603 cm<sup>-1</sup>. Stretching and bending vibrations of -N-H are observed at 3300 and 1533 cm<sup>-1</sup> respectively. In the FT-IR spectrum of PMMA-*b*-PU-*b*-PMMA tri-block copolymer, the stretching vibrations of urethane groups and ester carbonyl groups of PMMA blocks with increased intensity merged and appear at 1737 cm<sup>-1</sup>. The -C-H stretching vibrations of aromatic and aliphatic -CH in PU and PMMA are observed in the region 2851–3010 cm<sup>-1</sup> and -N-H stretching vibrations are observed in the region 3353–3550 cm<sup>-1</sup>. The stretching and bending vibrations of aromatic -C=C- (derived from TPE and TDI) are appeared at 1660 and 991 cm<sup>-1</sup> respectively. Methine out-of-plane bending vibrations of -C=C-H present in aromatic rings of TDI and TPE groups appeared at 749 cm<sup>-1</sup> and the stretching vibrations of ether -C-O-C- groups are observed at 1136 cm<sup>-1</sup>. The stretching vibrations of -C-N- and -C-O- present in -NHCOO- groups and PMMA blocks appeared at 1233 and 1275 cm<sup>-1</sup> respectively. The new peak appeared at 490 cm<sup>-1</sup> is due to the stretching vibrations of terminal C-Br groups which were formed during the reverse ATRP of MMA. The -C-H bending vibrations of methylene groups present in PU and PMMA are observed from 1439 to 1485 cm<sup>-1</sup>. The peak corresponding to -C-H bending vibrations of -CH<sub>3</sub> groups present in PU blocks (from TDI) and

PMMA blocks is observed at 1391 cm<sup>-1</sup>. The presence of all peaks corresponds to PU-TPE in tri-block copolymer and appearance of new peaks corresponds to PMMA blocks (cf. Table 4) further support the probable formation of PMMA-*b*-PU-*b*-PMMA tri-block copolymers.

### 3.3. Thermal studies

The PMMA-*b*-PU-*b*-PMMA tri-block copolymer obtained at 6 h (Table 2, POLY 3) was characterized by DSC. As shown in Figure 9, the  $T_g$  of the polyol segment present in PU-TPE and PMMA-*b*-PU-*b*-PMMA tri-block copolymers is observed at -59 and -61°C respectively. The  $T_g$  of the PMMA block is observed at 120°C which is more or less similar to the literature value of PMMA with the tacticity ratio of *rr:mr:mm* = 54:39:7 [34]. The presence of glass transition temperatures of soft and

**Figure 9.** DSC curves of (a) PU-TPE and (b) PMMA-*b*-PU-*b*-PMMA tri-block copolymer POLY 3

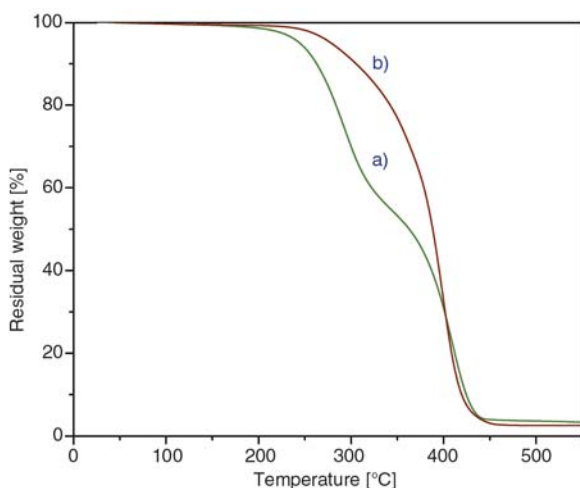


**Figure 10.** TGA curves of (a) PU-TPE and (b) PMMA-*b*-PU-*b*-PMMA tri-block copolymer POLY 3

hard segments may be taken as an evidence for the formation of PMMA-*b*-PU-*b*-PMMA tri-block copolymers. Thermal stability of PU-TPE and PMMA-*b*-PU-*b*-PMMA tri-block copolymer (Table 2, POLY 3) was studied and the results are presented in Figure 10. PU-TPE undergoes two-stage decomposition; one is around 284°C which is due to the decomposition of the NHCOO groups and another is around 404°C which is due to the decomposition of PTMG blocks. In the case of tri-block copolymers, the decomposition is not in stages but the overall thermal stability of PMMA-*b*-PU-*b*-PMMA tri-block copolymers is higher than the PU-TPE. Thermal degradation of standard radically prepared PMMA under nitrogen atmosphere proceeds in three steps corresponding to the cleavage of the head-to-head linkage (~165°C), the chain-end initiation from the vinylidene ends (~270°C), and random scission within the polymer chain (~360°C) [35]. Thermal degradation of the polymers synthesized using present initiating system occurred around 400°C which shows the presence random scission only. Similar type of results has been reported by Granel *et al.* for the controlled radical polymerization of methacrylic monomers in the presence of Ni(II) complex [36]. This result further indicates absence of abnormal linkages in the tri-block copolymers and confirms virtual absence of irreversible termination reactions.

#### 4. Conclusions

For the first time polyurethane-based macroiniferter, PU-TPE has been used to synthesize PMMA-*b*-

PU-*b*-PMMA tri-block copolymers through reverse ATRP. This is the first example of the synthesis of tri-block copolymers through reverse ATRP. ‘Living’ nature of the propagating radicals was further confirmed by time- $\ln([M]_0/[M])$  and conversion- $\overline{M}_n$  kinetic plots.  $\overline{M}_{n,th}$  of the tri-block copolymers was found to be more or less similar to  $\overline{M}_{n,GPC}$ . The molar percentage of PMMA calculated through  $^1\text{H NMR}$  is matching with GPC results. The results from spectral and thermal studies support the formation of PU-TPE and PMMA-*b*-PU-*b*-PMMA tri-block copolymers.

#### Acknowledgements

The authors would like to thank Council of Scientific and Industrial Research (CSIR), New Delhi, India for financial support to this project (No. 01(1964)/05/EMR-II dated 12<sup>th</sup> April, 2005).

#### References

- [1] Szwarc M.: ‘Living’ polymers. *Nature*, **176**, 1168–1169 (1956).
- [2] Szwarc M., Levy M., Milkovich R.: Polymerization initiated by electron transfer to monomer. A new method of formation of block copolymers. *Journal of American Chemical Society*, **78**, 2656–2657 (1956).
- [3] Matyjaszewski K., Kubisa P., Penczek S.: Kinetics and mechanism of the cationic polymerization of tetrahydrofuran in solution. 1. THF- $\text{CCl}_4$  system. *Journal Polymer Science, Part A: Polymer Chemistry*, **13**, 763–784 (1975).
- [4] Otsu T., Yoshida M.: Role of initiator-transfer agent-terminator (iniferter) in radical polymerizations: Polymer design by organic disulfides as iniferters. *Makromolekulare Chemie Rapid Communication*, **3**, 127–132 (1982).
- [5] Webster O. W.: Living polymerization methods. *Science*, **251**, 887–893 (1991).
- [6] Wayland B. B., Poszmik G., Mukerjee S. L., Fryd M.: Living radical polymerization of acrylates by organocobalt porphyrin complexes. *Journal of American Chemical Society*, **116**, 7943–7944 (1994).
- [7] Steenbock M., Klapper M., Müllen K.: Triazoliny radicals new additives for controlled radical polymerization. *Macromolecular Chemistry and Physics*, **199**, 763–769 (1998).
- [8] Moad G., Rizzardo E., Thang S. H.: Radical addition fragmentation chemistry in polymer synthesis. *Polymer*, **49**, 1079–1131 (2008).
- [9] Fischer H.: The persistent radical effect: A principle for selective radical reactions and living radical polymerizations. *Chemical Reviews*, **101**, 3581–3610 (2001).

- [10] Chung T. C., Janvikul W., Lu H. L.: A novel 'stable' radical initiator based on the oxidation adducts of alkyl-9-BBN. *Journal of American Chemical Society*, **118**, 705–706 (1996).
- [11] Braunecker W. A., Itami Y., Matyjaszewski K.: Osmium mediated radical polymerization. *Macromolecules*, **38**, 9402–9404 (2005).
- [12] Matyjaszewski K., Xia J.: Atom transfer radical polymerization. *Chemical Reviews*, **101**, 2921–2990 (2001).
- [13] Kamigaito M., Ando T., Sawamoto M.: Metal-catalyzed living radical polymerization. *Chemical Reviews*, **101**, 3689–3745 (2001).
- [14] Zhu Y. J., Tan Y. B., Du X.: Preparation and self-assembly behavior of polystyrene-block-poly (dimethylaminoethyl methacrylate) amphiphilic block copolymer using atom transfer radical polymerization. *Express Polymer Letters*, **2**, 214–225 (2008).
- [15] Barim G., Demirelli K., Coskun M.: Conventional and atom transfer radical copolymerization of phenoxycarbonylmethyl methacrylate-styrene and thermal behavior of their copolymers. *Express Polymer Letters*, **1**, 535–544 (2007).
- [16] Chen X-P., Qiu K-Y.: Synthesis of well-defined polystyrene by radical polymerization using 1,1,2,2-tetraphenyl-1,2-ethanediol/FeCl<sub>3</sub>/PPh<sub>3</sub> initiating system. *Journal of Applied Polymer Science*, **77**, 1607–1613 (2000).
- [17] Wang J-S., Matyjaszewski K.: 'Living'/controlled radical polymerization. Transition-metal-catalyzed atom transfer radical polymerization in the presence of a conventional radical initiator. *Macromolecules*, **28**, 7572–7573 (1995).
- [18] Xia J., Matyjaszewski K.: Homogeneous reverse atom transfer radical polymerization of styrene initiated by peroxides. *Macromolecules*, **32**, 5199–5202 (1999).
- [19] Li P., Qiu K-Y.: Copper(II) compound catalyzed living radical polymerization of methyl methacrylate in the presence of benzoyl peroxide. *Macromolecules*, **35**, 8906–8908 (2002).
- [20] Anand V., Agarwal S., Greiner A., Choudhary V.: Synthesis of methyl methacrylate and N-aryl itaconimide block copolymers via atom-transfer radical polymerization. *Polymer International*, **54**, 823–828 (2005).
- [21] Braun D., Becker K. H.: Aromatische Pinakole als Polymerisationsinitiatoren. *Die Angewandte Makromolekulare Chemie*, **6**, 186–189 (1969).
- [22] Tharanikkarasu K., Radhakrishnan G.: Tetraphenyl-ethane iniferters. 3. 'Living' radical polymerization of methyl methacrylate using toluene-diisocyanate-based polyurethane iniferter. *Journal of Macromolecular Science, Part A: Pure and Applied Chemistry*, **33**, 417–437 (1996).
- [23] Qin D-Q., Qin S-H., Chen X-P., Qiu K-Y.: Living/controlled radical polymerization of methyl methacrylate by reverse ATRP with DCDPS/FeCl<sub>3</sub>/PPh<sub>3</sub> initiating system. *Polymer*, **41**, 7347–7353 (2000).
- [24] Qin D-Q., Qin S-H., Qiu K-Y.: A reverse ATRP process with a hexasubstituted ethane thermal iniferter diethyl 2,3-dicyano-2,3-di(*p*-tolyl)succinate (DCDTS) as the initiator. *Macromolecules*, **33**, 6987–6992 (2000).
- [25] Chen X-P., Qiu K-Y.: Synthesis of well-defined poly(methyl methacrylate) by radical polymerization with a new initiation system TPED/FeCl<sub>3</sub>/PPh<sub>3</sub>. *Macromolecules*, **32**, 8711–8715 (1999).
- [26] Li P., Qiu K-Y.: Reverse atom transfer radical polymerization of styrene in the presence of tetraethylthiuram disulfide. *Polymer*, **43**, 3019–3024 (2002).
- [27] Kim B. K., Tharanikkarasu K., Lee J. S.: Polyurethane-polymethacrylic acid multi-block copolymer dispersions through polyurethane macroiniferters. *Colloid and Polymer Science*, **277**, 285–290 (1999).
- [28] Tharanikkarasu K., Radhakrishnan G.: Tetraphenyl-ethane iniferters-9. Diphenylmethane diisocyanate-based polyurethane-polystyrene block copolymers through 'living' radical mechanism. *European Polymer Journal*, **33**, 1779–1786 (1997).
- [29] Tharanikkarasu K., Radhakrishnan G.: Tetraphenyl-ethane iniferters: Polyurethane-polystyrene multi-block copolymers through 'living' radical polymerization. *Journal of Applied Polymer Science*, **66**, 1551–1560 (1997).
- [30] Braunecker W. A., Matyjaszewski K.: Recent mechanistic developments in atom transfer radical polymerization. *Journal of Molecular Catalysis, A: Chemical*, **254**, 155–164 (2006).
- [31] Destarac M., Matyjaszewski K., Boutevin B.: Polychloroalkane initiators in copper-catalyzed atom transfer radical polymerization of (meth)acrylates. *Macromolecular Chemistry and Physics*, **201**, 265–272 (2000).
- [32] Wang J-S., Matyjaszewski K.: Controlled/'living' radical polymerization. Halogen atom transfer radical polymerization promoted by a Cu(I)/Cu(II) redox process. *Macromolecules*, **28**, 7901–7910 (1995).
- [33] Higaki Y., Otsuka H., Takahara A.: Facile synthesis of multiblock copolymers composed of poly(tetramethylene oxide) and polystyrene using living free-radical polymerization macroinitiator. *Polymer*, **47**, 3784–3791 (2006).
- [34] Brandrup J., Immergut E. H., Grulke E. A.: *Polymer handbook*. John Wiley and Sons, Toronto (1989).
- [35] Hatada K., Kitayama T., Fujimoto N., Nishiura T.: Stability and degradation of polymethacrylates with controlled structure. *Journal of Macromolecular Science, Part A: Pure and Applied Chemistry*, **30**, 645–667 (1993).
- [36] Granel C., Dubois P., Jérôme R., Teyssié P.: Controlled radical polymerization of methacrylic monomers in the presence of a bis(ortho-chelated) aryl-nickel(II) complex and different activated alkyl halides. *Macromolecules*, **29**, 8576–8582 (1996).